

# APPLICATION OF TRANSIENT PRESSURE ANALYSIS TO WELLS WITH HYDRAULICALLY INDUCED VERTICAL FRACTURES

JAMES T. SMITH  
Texas Tech University  
WILLIAM M. COBB  
Cornell Oil Company

## ABSTRACT

*Since the inception in 1947 of hydraulic fracturing as a method of stimulating oil and gas wells, fractured wells have become commonplace throughout the world. This is particularly true in regions noted for low permeability and accompanying low productivity. Transient pressure tests conducted in fractured reservoirs are subject to unconventional behavior which requires special interpretational skills and procedures. The purpose of this paper is to discuss those methods of pressure analysis which have been most successfully applied to wells that intersect single-plane vertical fractures.*

*Procedures for evaluating reservoir permeability, formation damage, and fracture length are presented for both conventional and type-curve methods of analysis. Practical tests and rules-of-thumb which will help an engineer avoid common pitfalls in fractured well analysis are presented. Both infinite- and finite-conductivity fractures are discussed.*

## INTRODUCTION

Transient pressure testing has experienced widespread use for approximately three decades as a method of obtaining reservoir properties, analyzing reservoir behavior, and monitoring the performance of injection and production wells. Numerous papers and three monographs<sup>1, 2, 3</sup> have been written during this period to deal with various aspects of well-testing technology. Most of this technology has been directed toward rather simplified reservoirs in which fluid was assumed to flow radially along paths that converge at the test well.

Hydraulic fracturing has been an effective method of stimulating oil and gas wells since its introduction to the petroleum industry in 1947. It was recognized early<sup>4, 5, 6</sup> that a fracture significantly alters the flow patterns and, consequently, alters the pressure behavior of a reservoir which contains a fracture. For this reason,

conventional methods<sup>7, 8, 9</sup> of analyzing pressure data had to be modified to account for the presence of a fracture.

The first major breakthrough in fracture-well analysis was made by Russell and Truitt.<sup>10</sup> They presented a method of analyzing pressure data, based on the Horner<sup>7</sup> plot; the method applied to fully penetrating vertical fractures with infinite conductivity. It was shown that a Horner plot does not behave for fractured wells as it does for non-fractured wells but, by applying appropriate correction factors, this long-used method could still be used. While improvements and adaptations have been made since its publication in 1961, this paper still serves as the basis of most conventional fractured well analyses.

In a study of pressure-falloff testing, Clark<sup>11</sup> extended the work of Russell and Truitt to include fractured injection wells. He showed that a cartesian plot of  $P_{ws}$  vs  $\Delta t^{1/2}$ , based on linear flow theory, could be combined with a plot of  $P_{ws}$  vs  $\log \Delta t$ , based on radial flow theory, to obtain an estimate of reservoir flow capacity and fracture length. A method was also suggested which can be used to directly obtain the pressure loss due to skin effects from the square root plot.

Fracture well analysis was extended to gas wells by Millheim and Cichowicz<sup>12</sup> in 1968. It was shown by these authors, and by Wattenbarger and Ramey<sup>13</sup>, that non-darcy flow can alter the pressure behavior of fractured wells and, in particular, can cause errors in calculated values of formation flow capacity.

The concept of applying type curves to pressure analysis, introduced by Agarwal, et al.<sup>14</sup> for radial

flow systems, was extended to fractured wells by Raghavan, Cady and Ramey<sup>15</sup>. The application of type-curve matching methods to fractured wells actually began, however, in 1974 with the publication<sup>16, 17, 18</sup> of type curves for infinite-conductivity vertical fractures and for both vertical and horizontal fractures with uniform flux. The combination of conventional and type-curve methods resulted in a much higher level of confidence in calculated results.

While transient pressure testing has been very successful in many wells, problems often arise if the objective of the test is to determine fracture length or to evaluate formation damage. The majority of pressure tests in fractured wells are analyzed using methods which assume the fracture to have infinite conductivity. This assumption, however, often results in calculated fracture lengths which are significantly less than design lengths. This discrepancy has led researchers to recognize that many fractures have finite flow capacity and cannot be adequately evaluated using analysis techniques which assume infinite fracture conductivity. Accordingly, solutions for finite-capacity fractures have been developed.<sup>19, 20</sup>

Solutions for finite-capacity fractures are more complex than for the infinite-capacity systems because of the additional variable of fracture capacity; further, they are more difficult to apply. Attempts to use finite capacity solutions have resulted in none-unique answers and have led to erroneous conclusions.

The purpose of this paper is to discuss those methods of analysis, both conventional and type curve, which are most widely used. Procedures and equations necessary to evaluate formation flow capacity, formation damage, and fracture length are presented. Emphasized are practical rules-of-thumb which will help the engineer avoid common pitfalls in fracture well analysis. Both infinite and finite conductivity fractures are discussed. Whereas the methods presented are generally applicable to various types of well tests, this discussion is limited to the analysis of pressure buildup tests.

### PRESSURE BUILDUP ANALYSIS IN UNFRACTURED WELLS

It is instructive to review some basic concepts of pressure buildup testing in unfractured reservoirs.

The technology used to analyze pressure buildup data from wells in unfractured reservoirs has long been established.<sup>7, 8</sup> Horner<sup>7</sup> showed that if a well is flowed at constant rate for a time  $t$  and is then shut in for a buildup test, the static formation-face pressure after a shut-in time  $\Delta t$  can be predicted by the following relationship.

$$P_{ws} = p^* - \frac{162.6 qB\mu}{kh} \log \frac{t + \Delta t}{\Delta t} \quad (1)$$

This equation represents an idealized reservoir in which formation thickness, porosity, permeability, fluid viscosity and fluid compressibility are assumed to be constant. It is further assumed that the reservoir contains a single-phase fluid which flows radially toward the wellbore at a rate which results in small pressure gradients that can be described by radial flow theory.

Equation 1 suggests that a plot of  $P_{ws}$  vs  $\log \frac{t + \Delta t}{\Delta t}$  will yield a straight line having a slope  $m$  according to the following equation.

$$m = \frac{162.6 qB\mu}{kh} \quad (2)$$

This relationship is illustrated by the Horner plot in Figure 1.

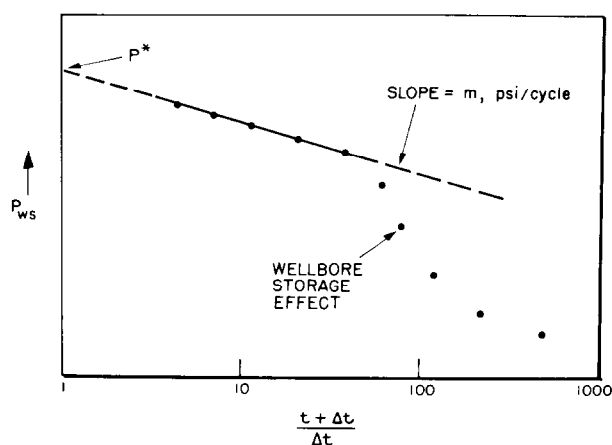


FIGURE 1 - CONVENTIONAL HORNER PLOT FOR A WELL WITH RADIAL FLOW

After the proper straight line has been identified and its slope has been determined, the formation capacity can be computed as follows.

$$kh = \frac{162.6 qB\mu}{m} \quad (3)$$

If a reliable value of formation thickness is available, it is obvious that the average permeability can also be computed using Equation 3.

### FORMATION DAMAGE

One of the most useful applications of a pressure buildup test is to diagnose a well for possible formation damage. Van Everdingen and Hurst<sup>21,22</sup> showed that formation damage can be quantified in terms of a dimensionless pressure loss referred to as the skin factor. The skin factor  $s$  can be computed using the following equation.

$$s = 1.151 \left[ \frac{p_{1hr} - p_{wf}}{m} - \log \frac{k}{\phi \mu c r_w^2} + 3.23 \right] \quad (4)$$

Here,  $p_{1hr}$  is obtained from the Horner straight line, or its extension, at a shut-in time of one hour, and  $p_{wf}$  is the flowing bottomhole pressure at the time of shut-in. The log term in Equation 4 has an approximate value of 8 for any combination of rock and fluid properties encountered in practice. Consequently, if  $k$ ,  $\phi$ ,  $\mu$ ,  $c$ , and  $r_w$  are not known with a high degree of confidence, Equation 4 can be used in the following simplified form with little loss of accuracy.

$$s = 1.151 \left[ \frac{p_{1hr} - p_{wf}}{m} - 5 \right] \quad (5)$$

When the concept of the skin factor was initially published, it was reported that a positive value of  $s$  indicates formation damage, whereas a negative value reflects formation stimulation. Unfortunately, this oversimplified interpretation of the skin factor is still adhered to by many engineers and results each year in numerous incorrect engineering decisions.

A positive value of skin does not necessarily mean a well is damaged. Any flow restriction in the reservoir near the test well which causes a pressure

loss not accounted for by ideal radial flow theory will result in a calculated skin factor greater than zero. This restriction may be formation damage, but it can also result from other factors such as turbulence, perforations, partial penetration, and gas blockage. The total skin factor  $s$ , therefore, is in reality a composite of several of the following skin factors.

$$s = s_{dam} + s_{pen} + s_{perf} + s_{turb} + s_{frac} + s_{swp} \quad (6)$$

where

- $s_{dam}$  = skin due to permeability alteration; this includes formation damage
- $s_{pen}$  = skin due to a partially opened interval
- $s_{perf}$  = skin due to perforations
- $s_{turb}$  = skin due to turbulence
- $s_{frac}$  = skin due to fracture
- $s_{swp}$  = skin due to slanted well

If the purpose of a pressure test is to determine if a formation is damaged, it is evident from Equation 6 and  $s_{dam}$  not  $s$ , needs to be evaluated. The total skin  $s$  may be a large positive number while  $s_{dam}$  is zero. This fact is often misunderstood and has resulted in many unnecessary stimulation treatments. The estimation of  $s_{dam}$  requires, however, that other skin factors in Equation 6 be known. This can be a difficult task but methods are available<sup>2</sup> to estimate these quantities.

Being a dimensionless number, the skin factor reveals the presence of a flow restriction but it does not clearly indicate the magnitude of the restriction. The pressure loss caused by the skin is directly proportional to the production rate as expressed by the following relationship.

$$\Delta p_{skin} = \frac{141.2 qB\mu}{kh} s = 0.87 ms \quad (6)$$

The flow efficiency is as follows.

$$FE = \frac{\bar{p} - p_{wf} - \Delta p_{skin}}{\bar{p} - p_{wf}} \quad (7)$$

When  $\bar{p}$  is not known, it is generally sufficient to approximate the flow efficiency as the following.

$$FE \approx \frac{p^* - p_{wf} - \Delta p_{skin}}{p^* - p_{wf}} \quad (8)$$

Here,  $p^*$  is determined from the Horner straight line at a time ratio of unity, as illustrated by Figure 1.

If it is assumed that the skin factor used in Equations 7 or 8 can be removed by a stimulation treatment, and that  $p_{wf}$  is the same before and after stimulation, the flow rate after stimulation will be the following.

$$q_{\text{after}} = \frac{1}{FE} q_{\text{before}} \quad (9)$$

The value of FE used in Equation 9 should be based on  $s_{\text{dam}}$ , not  $s$ . The increase in flow rate predicted by Equation 9 permits an engineer to determine beforehand if a proposed stimulation expenditure is justified.

### WELLBORE STORAGE

The foregoing discussion may indicate pressure-buildup analysis is simple. It is simple, but only after the proper Horner straight line has been identified. Most wells tested are subject to flow behavior which violates one or more of the assumptions upon which Equations 1-3, and Figure 1, are based. Consequently, buildup data on a Horner plot may form not one, but several straight lines. The most difficult problem faced by the engineer is to determine which line represents true reservoir behavior.

The most commonly occurring problem that affects buildup behavior is wellbore storage. Equation 1 assumes that flow from the formation stops instantaneously at the time of shut-in. In practice, a well is shut-in at the surface, and fluids continue to enter the wellbore after the buildup test has begun. This "afterflow" violates one of the basic assumptions in Equation 1 and leads to the result that early time pressures will be less than those predicted by Equation 1. When afterflow ceases, measured pressures fall on the predicted Horner straight line.

Data affected by wellbore storage may form a straight line on the Horner plot. If this line is mistakenly chosen as the Horner straight line, subsequent calculations will be incorrect. This confusion, and the misinterpretations which follow, can be avoided if that segment of the data affected by storage can be identified.

Agarwal<sup>14</sup> showed that a log-log plot of  $(p_{ws} - p_{wf})$  versus  $\Delta t$  can be used to identify that part of the buildup data altered by wellbore storage. Those points *completely* controlled by storage will plot as a straight line having a unit slope; this is illustrated by Figure 2. Further, if the time  $\Delta t^*$  at which the unit slope line ends is determined, it can be expected that pressures measured after  $50 \Delta t^*$  will not be affected by storage; that is, the Horner straight line will begin at a time ratio corresponding to  $50 \Delta t^*$ . This is a very powerful interpretational tool, but it does require that an accurate value of producing pressure,  $p_{wf}$ , and early time buildup pressures,  $p_{ws}$ , be measured.

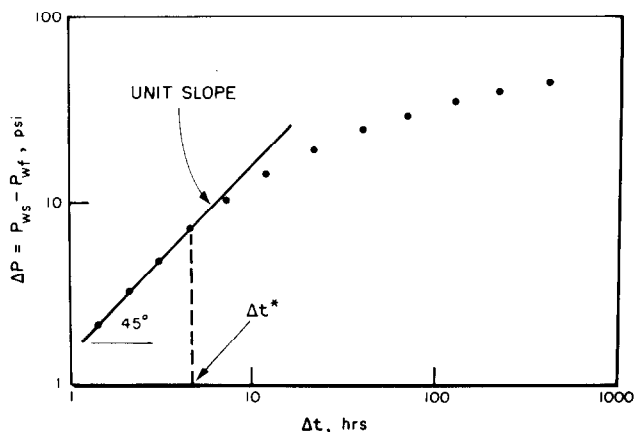


FIGURE 2—LOG-LOG PLOT SHOWING EFFECT OF WELLBORE STORAGE

It will be shown in the next section that pressure data from fractured reservoirs is affected by wellbore storage in the same way as data from nonfractured formations.

### INFINITE CONDUCTIVITY FRACTURES

While it is recognized that there are several different types of fractured reservoirs, hydraulic fracturing accounts for the majority of fractured systems. Most hydraulic fractures are vertical and fully penetrate the formation, as illustrated by Figure 3. Fractures are further categorized by their conductivity. Infinite conductivity fractures are those in which the fluid pressure is constant along the fracture at any given time; that is, there is no pressure loss in the fracture. Although pressure may change with time in an infinite-conductivity fracture, it does not change with position along the fracture.

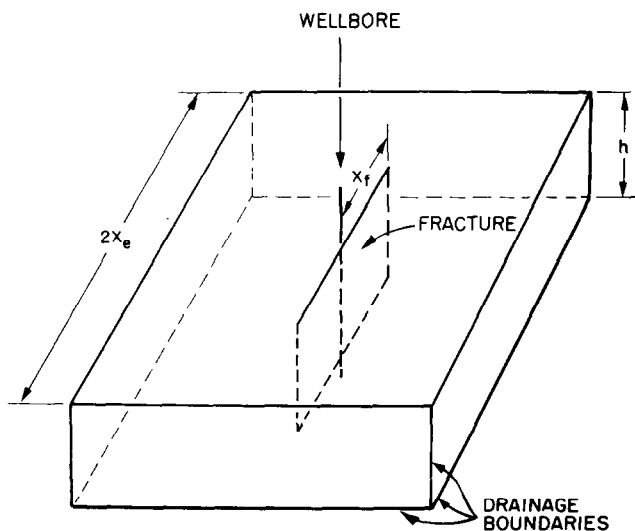


FIGURE 3—SCHEMATIC OF A FRACTURED WELL AND THE ASSOCIATED DRAINAGE AREA

When a reservoir is fractured, the pressure behavior can no longer be described by conventional radial-flow theory. Instead, it has been shown that pressures exhibit linear flow behavior at early test times, and pseudoradial behavior at later times. Both of these flow periods yield valuable reservoir information.

### LINEAR FLOW

It is suggested by pressure-drawdown theory that buildup pressures at early test times can be described by the following linear flow relationship.

$$P_{ws} = p_{wf} + \frac{16.3qB}{A_f} \left[ \frac{\mu\Delta t}{\phi ck} \right]^{1/2} + \frac{141.2 qB\mu (s-s_{frac})}{kh} \quad (10)$$

Equation 10 indicates that a plot of  $P_{ws}$  versus  $\Delta t^{1/2}$  will produce a straight line during the period of linear flow; this is illustrated by Figure 4. Furthermore, if the skin is negligible, taking the logarithm of Equation 10 yields the following expression.

$$\log(p_{ws} - p_{wf}) = \log \left[ \frac{16.3 qB}{A_f} \left( \frac{\mu}{\phi ck} \right)^{1/2} \right] + \frac{1}{2} \log \Delta t \quad (11)$$

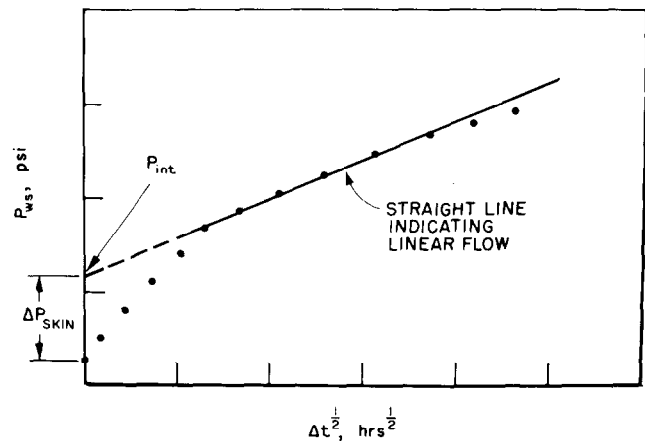


FIGURE 4—SQUARE ROOT PLOT SHOWING THE EFFECT OF LINEAR FLOW

The form of Equation 11 suggests that a plot of  $(p_{ws} - p_{wf})$  versus  $\Delta t$  on log-log paper will trace a straight line. Moreover, it is significant that the slope of this line will be  $0.5$  ( $26^\circ$ ). This relationship is illustrated by Figure 5. If severe skin is present, however, the log-log graph will yield a slope much less than one-half at early times. Raghavan<sup>23</sup> discusses this idea and suggests that it is a qualitative method for identifying damage on the fracture face.

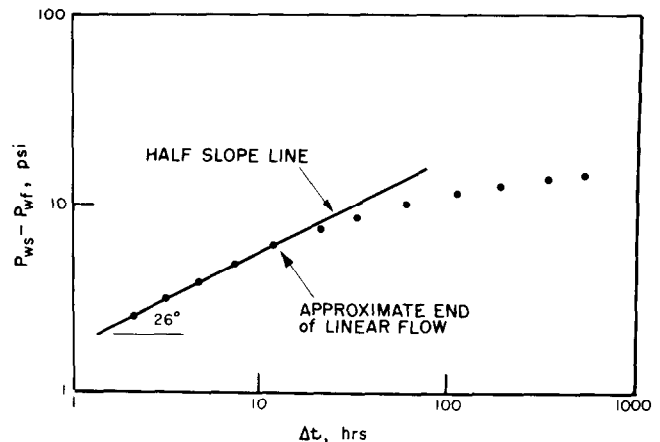


FIGURE 5—LOG-LOG PLOT SHOWING THE EFFECT OF LINEAR FLOW

The straight line relationships illustrated by Figures 4 and 5 provide distinctive and easily recognizable evidence of a fracture. When properly applied, these graphs are one of the best diagnostic tools available to the engineer for the purpose of detecting a fracture.

When the duration of the linear-flow period is short, as it often is, care must be taken not to

misinterpret the data. It is common in this situation for skin effects or wellbore storage effects to alter pressures to the extent that the linear flow data cannot be recognized. Interpretation in such cases is difficult. This problem will be discussed in greater detail in a subsequent section.

### PSEUDORADIAL FLOW

Following the period of linear pressure behavior, and a transition period, pressures begin to exhibit characteristics similar to a radial flow system; hence, this period is referred to as pseudoradial flow. The pressure behavior during this time is very dependent upon fracture penetration; that is, flow is almost radial for short fracture lengths, but becomes linear as the fracture length increases to the drainage radius of the well. This dependence upon fracture length is illustrated by the theoretical Horner buildup curves of Russell and Truitt presented in Figure 6. Note that fracture penetration is expressed as a ratio of fracture length,  $x_f$ , to the drainage radius,  $x_e$ , of the subject well.

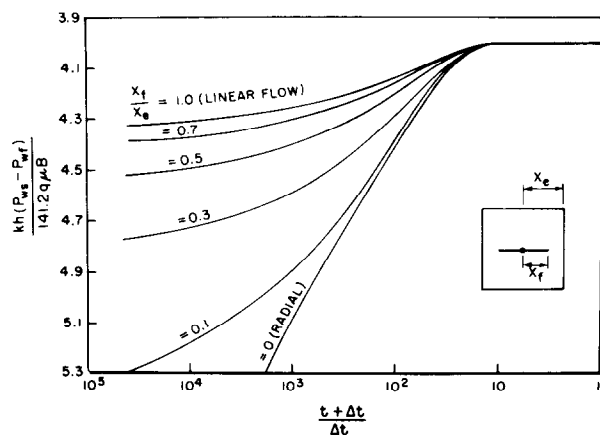


FIGURE 6—THEORETICAL BUILDUP CURVES OF RUSSELL AND TRUITT<sup>10</sup>

Some very important observations can be made from Figure 6. First, the effect of fracture penetration on the Horner plot is obvious; the buildup behavior varies from radial to linear as fracture length increases. Second, there is no true straight line on any of the fracture curves; however, each curve develops a maximum slope which approaches the slope of the radial case as fracture length decreases. Finally, if it is not recognized that a well is fractured, and the maximum slope of the Horner plot is selected for analysis by conventional

radial flow techniques, the slope will always be too small. Formation characteristics can be correctly determined from the Horner plot only if the slope used is the same as that indicated by the radial flow curve. It is observed, however, that the fracture curves always have a maximum slope less than the radial case. Further, the error increases as fracture length increases. Obviously, the Horner plot cannot be applied to fractured reservoirs in the same manner as it is used to analyze nonfractured systems.

### PERMEABILITY AND FRACTURE LENGTH

The most commonly used approach to fracture well analysis requires, the use of two graphs: (1) a cartesian plot of  $P_{ws}$  vs  $\Delta t^{1/2}$ , and (2) a Horner plot. It was shown previously that the buildup pressures,  $P_{ws}$ , will form a straight line on the square root plot during that time period in which linear flow is dominant. It can be shown<sup>11</sup> from Equation 10 that the slope of this line,  $m_1$ , is equal to the following expression.

$$m_1 = \frac{4.07 qB}{x_f h} \left[ \frac{\mu}{\phi c k} \right]^{1/2} \quad (12)$$

Thus,

$$x_f = \frac{4.07 qB}{m_1 h} \left[ \frac{\mu}{\phi c k} \right]^{1/2} \quad (13)$$

Equation 13 relates fracture length to permeability; if either quantity is known from another source, this equation can be used to compute the unknown information.

The maximum slope on the Horner plot,  $m$ , will not give the true reservoir permeability, but it can be used to compute an apparent permeability according to the familiar equation.

$$k_a = \frac{162.6 qB\mu}{m'h} \quad (14)$$

Significantly, it was shown by Russell and Truitt<sup>10</sup> that the apparent permeability can be corrected for fracture penetration,  $x_f/x_e$ , as follows to obtain the true permeability.

$$k = RK_a = \frac{162.6 qB\mu}{m'h} R \quad (15)$$

The correction factor, R, is a function of fracture penetration according to the correlation presented in Figure 7.

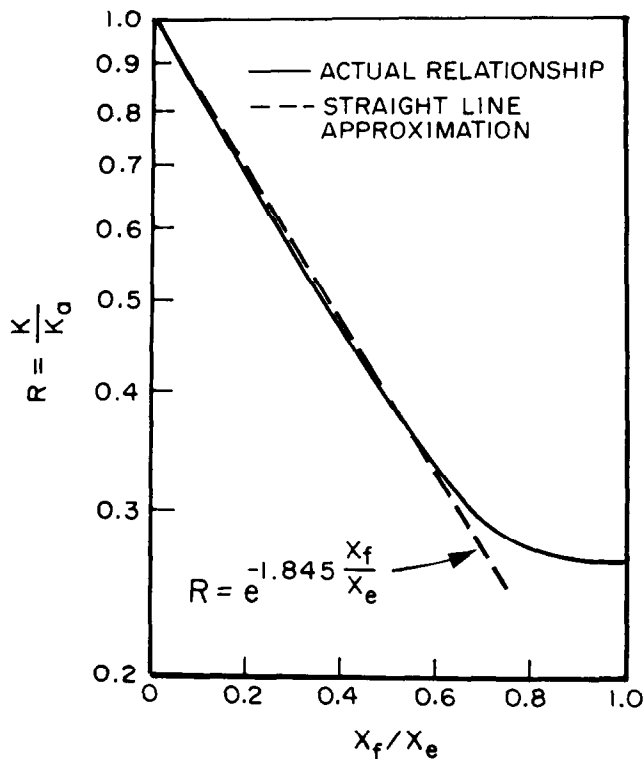


FIGURE 7—PERMEABILITY CORRECTION FACTOR FOR PRESSURE BUILDUP TESTS IN VERTICALLY FRACTURED WELLS. AFTER RUSSELL & TRUITT.<sup>10</sup>

This plot shows that R is a straight line function of fracture penetration for values of  $x_f/x_e$  less than about 0.7. The straight line portion of this curve can be approximated by the following relationship.

$$R = \text{Exp} \left[ -1.845 \frac{x_f}{x_e} \right] \quad (16)$$

A correlation for R was also developed by Raghavan, et al.<sup>15</sup>, but was found to differ insignificantly from Figure 7.

Equations 13 and 15 can be combined to obtain the following equation.

$$x_f = \frac{0.319}{m_1} \left[ \frac{m' qB}{\phi chR} \right]^{1/2} \quad (17)$$

This expression can be solved for  $x_f$  and k using the following procedure.

1. Assume a value of  $x_f$ ;
2. Determine R using Equation 16 or Figure 7;
3. Compute  $x_f$  using Equation 17;
4. Repeat steps 1-3 until the assumed and calculated values of  $x_f$  are equal;
5. Compute k using Equation 15.

An example which illustrates this procedure is presented in a subsequent section.

### FORMATION DAMAGE

If the slope of the Horner plot is corrected for fracture penetration, i.e.,  $m = m'/R$ , Equation 4 can be used to compute the total skin factor. Recall, however, that the total skin is a composite of several skin factors as defined by Equation 6. The dominant skin term in a fractured well is generally  $s_{frac}$ . Due to the stimulation effect of the fracture,  $s_{frac}$  will be a large negative number; consequently, s will generally be a negative number.

An accurate evaluation of formation damage requires that  $s_{dam}$  be known. In order to compute  $s_{dam}$  from Equation 6,  $s_{frac}$  must be determined from an independent source. With current technology, there is no reliable method for determining  $s_{frac}$ . Accordingly, the skin due to damage cannot be evaluated using Equations 4 and 6.

The total skin factor exclusive of  $s_{frac}$ , i.e.,  $s-s_{frac}$ , can be determined from the square root plot illustrated by Figure 4. According to Equation 10, extrapolation of the straight line on this graph to  $\Delta t^{1/2} = 0$  will result in an intercept,  $p_{int}$ , described as follows.

$$P_{int} = p_{wf} + \frac{141.2 qB\mu}{kh} (s-s_{frac}) \quad (18)$$

so that

$$s-s_{frac} = \frac{(p_{int} - p_{wf}) kh}{141.2 qB\mu} \quad (19)$$

The skin difference in Equation 19 has often been reported as  $s_{dam}$ . It is clear from Equation 6,

however, that this is true only when other flow restrictions are negligible. If the remaining skin factors can be evaluated, or neglected, this skin difference can be substituted into Equation 6 to obtain  $s_{dam}$ .

It is cautioned that an accurate value of  $p_{wf}$  is required to calculate  $s_{dam}$ ; this pressure should be measured at the time of shut-in. Any error in  $p_{wf}$  will be directly reflected in  $s_{dam}$ . Also, one must make sure that the straight line on the square root plot corresponds to linear flow. The data which form this line should also plot as a half-slope straight line on the log-log plot of  $(p_{ws} - p_{wf})$  versus  $\Delta t$ .

The log-log plot can also be valuable as a means of recognizing skin in a well. In the absence of skin and storage effects, an infinite-conductivity fracture causes early-time data to form a half-slope line on the log-log plot. However, if skin effects are present, the early time data will form a slope less than one-half. This is illustrated by Figure 8. Note on Figure 8 that skin causes the early-time data to approach the half-slope line from above. Unfortunately, if wellbore storage effects are also present, this observation does not apply; wellbore storage causes the log-log plot to have a slope greater than one-half at early times, thereby masking the presence of a skin in the well.

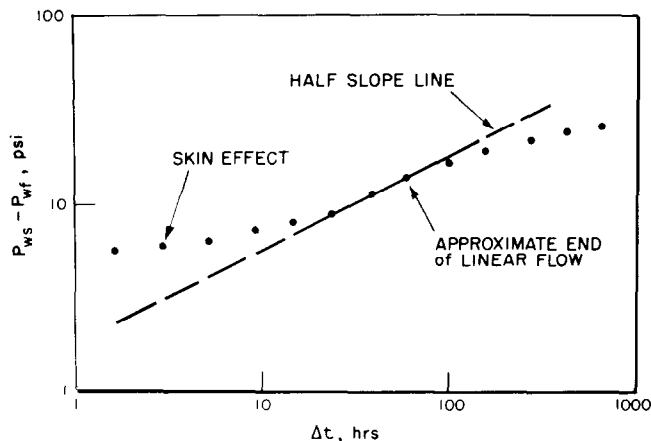


FIGURE 8—EFFECT OF SKIN ON THE LOG-LOG PLOT FOR A VERTICALLY FRACTURED WELL

## WELLBORE STORAGE

Wellbore storage affects buildup behavior in fractured systems much like it does in non-fractured reservoirs. Figure 9 is a log-log graph depicting buildup data from a fractured well with wellbore

storage. At early times when storage controls the data, a unit slope line is formed. As time increases, the data deviate from the unit slope line and approach asymptotically the line of half-slope. It is important to observe that a transition region exists between the unit slope and half-slope lines. If the linear flow period is short, or if wellbore storage effects are severe, the half-slope line may not appear.

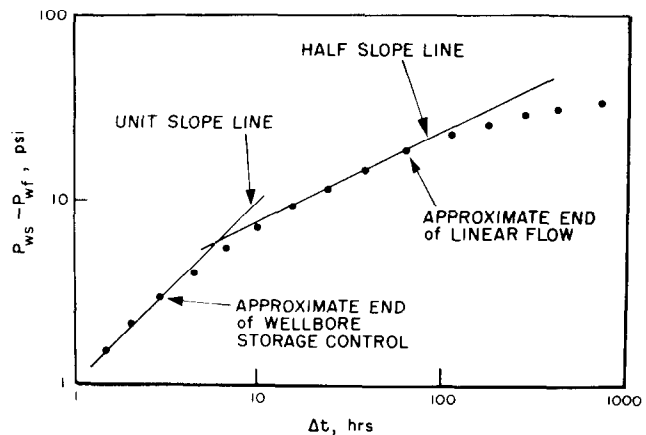


FIGURE 9—EFFECT OF WELLBORE STORAGE ON LOG-LOG PLOT FOR A VERTICALLY FRACTURED WELL

The importance of having an accurate value of  $P_{wf}$  is again emphasized; if  $p_{wf}$  is wrong, the value of  $(p_{ws} - p_{wf})$  used to prepare the log-log plot will be correspondingly wrong. This error will cause the shape and position of the curve to be incorrect. For example, data controlled by storage should plot as a unit slope line; if  $p_{wf}$  is too small, the storage data will plot instead as a curve concave upward with slope less than unity. This could easily lead an engineer to misinterpret the data as representing skin effects rather than wellbore storage.

## AVERAGE RESERVOIR PRESSURE

The volumetric average pressure in the drainage area of a test well is being determined<sup>10, 15</sup> by the Extended Muskat Method<sup>24</sup>. This method, illustrated by Figure 10, requires that  $\log(\bar{p} - p_{ws})$  versus  $\Delta t$  be plotted for assumed values of  $\bar{p}$ ; the minimum value of  $\bar{p}$  which results in a straight line relationship at large values of  $\Delta t$ , is the correct average pressure. The major disadvantage of this procedure is that long shut-in times are often required to obtain a solution. Minimum shut-in times required for this

method to be valid can be approximated<sup>15</sup> by the following expression.

$$\Delta t > \frac{190\phi\mu cA}{k} \quad (20)$$

If a Muskat analysis is made using data obtained before the minimum value of  $\Delta t$  is reached, a straight line may result but the value of  $\bar{p}$  will be incorrect.

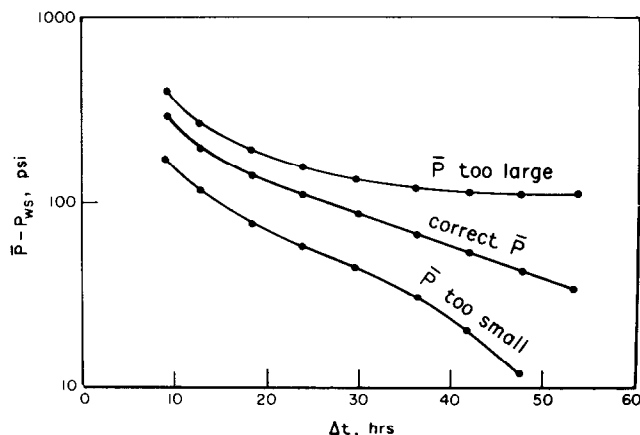


FIGURE 10—EXTENDED MUSKAT PLOT TO DETERMINE AVERAGE PRESSURE FROM PRESSURE BUILDUP DATA

### TYPE CURVE ANALYSIS

An alternate approach to fracture well analysis is to use “type curves.” This method, which has gained recent popularity, eliminates the trial-and-error procedure required by conventional analysis.

A type curve is a theoretical graph of pressure versus time on log-log paper. The type curve for an infinite conductivity fracture with no skin or storage effects is presented in Figure 11. Conveniently, both pressure and time are plotted in dimensionless form. Dimensionless time,  $\Delta t_{Dx_f}$  is related to real time by the following equation.

$$\Delta t_{Dx_f} = \frac{0.000264 k\Delta t}{\phi\mu c x_f^2} \quad (21)$$

Dimensionless pressure is defined as follows.

$$p_D = \frac{kh(p_{ws} - p_{wf})}{141.2 qB\mu} \quad (22)$$

While dimensionless numbers tend to confuse an engineer accustomed to working with real time and pressure, this method permits us to present on a single graph all of the theoretical buildup curves that apply to infinite conductivity fractures with no skin and storage.

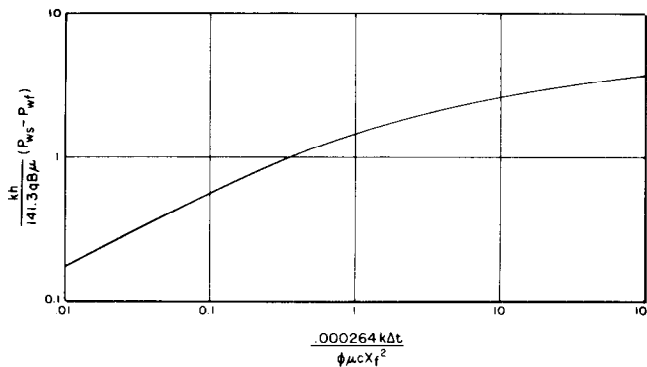


FIGURE 11—TYPE CURVE FOR INFINITE CAPACITY VERTICAL FRACTURE. AFTER AGARWAL.<sup>14</sup>

The use of Figure 11 to determine permeability and fracture length requires a curve matching procedure. First, prepare on tracing paper a log-log plot of  $(p_{ws} - p_{wf})$  versus  $\Delta t$  which has the same scale as the type curve. This curve is referred to as a “data curve.” Overlay the data curve onto the type curve and, keeping the major axes of the two graphs parallel, move the curves relative to each other until the best match is obtained. This procedure shows us which theoretical solution the particular set of field data matches. Since the characteristics of the theoretical solution are known, a match of the field data with the type curve permits determination of the properties of the reservoir from which the data were obtained.

After the best match of field data and theoretical data is obtained, select any point on the matched curves which is common to both curves. Determine from the data curve and type curve, respectively, the values of  $(p_{ws} - p_{wf})_m$  and  $p_{Dm}$  which define the match point. Substitute these values into Equation 22 and compute  $k$ .

$$k = \frac{141.2 qB\mu}{h} \frac{p_{Dm}}{(p_{ws} - p_{wf})_m} \quad (23)$$

Similarly, determine the values of  $\Delta t_m$  and  $(\Delta t_{Dx_f})_m$  which define the match point. Then, calculate  $x_f$ .

$$x_f = \left[ \frac{0.000264k}{\phi \mu c} \frac{\Delta t_m}{(\Delta t_{Dx_f})_m} \right]^{1/2} \quad (24)$$

The skin factor and average reservoir pressure must be determined using conventional methods previously described.

### EXAMPLE PROBLEM

A field example more fully illustrates these theoretical concepts. Water was injected into the Grayburg formation at an average rate of 350 BWPD for 8,540 hours. The well was then shut in for a 331 hour pressure falloff test. The bottom-hole injection pressure prior to shut in,  $p_{wi}$ , is 2,713 psi. The well is located in the center of a 40 acre 5-spot pattern resulting in wells on 20-acre spacing units. The effective injection well radius is 526 ft. Additional reservoir data are listed in Table 1. Well records indicate an initial acid stimulation treatment of 5000-10,000 gallons at treating pressures which exceed fracture pressures. Also, injection pressures have generally exceeded the formation fracture pressure. Consequently, there is reason to believe this is a fractured well.

TABLE 1—ROCK AND FLUID DATA FOR GRAYBURG RESERVOIR

$\phi$	= 8%
$c$	= $10 \times 10^{-6} \text{ psi}^{-1}$
$\mu_w$	= 0.8 cp
$h$	= 55 ft
$r_w$	= 0.33 ft.
$A$	= 20 Acres
$B_w$	= 1.0 RB/STB

Figure 12 presents a Horner graph of the test data. The maximum slope,  $m'$ , is 460 psi/cycle. From Equation 14, the apparent permeability to water is as follows.

$$k_a = \frac{(162.6) (350) (1) (0.8)}{(460) (55)}$$

$$k_a = 1.80 \text{ md}$$

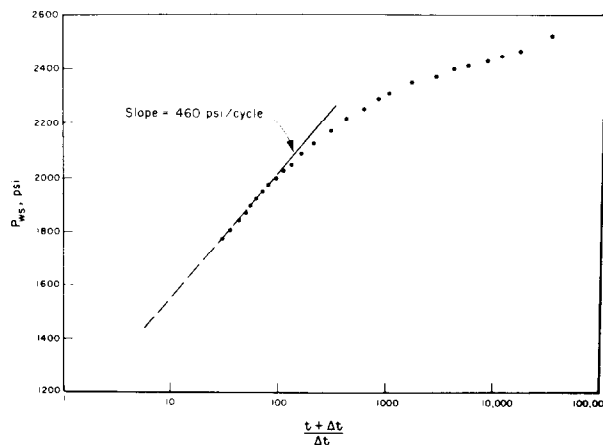


FIGURE 12—HORNER PLOT FOR EXAMPLE PROBLEM

This value must be corrected to obtain true permeability as indicated by Equation 15.

The pressure falloff test is analogous to the pressure buildup test; hence they can be analyzed using a similar procedure. The only difference in analyzing the two tests occurs when constructing the log-log plot; whereas it is necessary to plot  $(p_{ws} - p_{wi})$  for the buildup test, the falloff test requires that we plot  $(p_{wi} - p_{ws})$ . A log-log plot of  $(p_{wi} - p_{ws})$  vs  $\Delta t$  is presented in Figure 13.

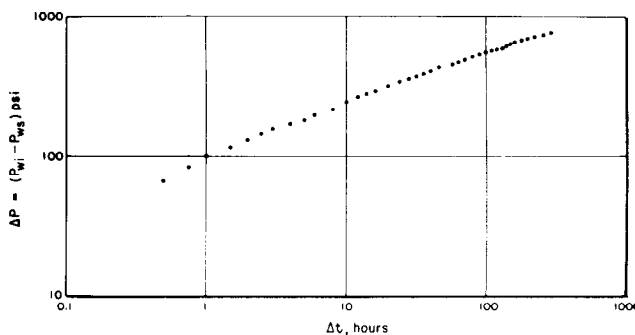


FIGURE 13—DATA CURVE FOR EXAMPLE PROBLEM

The initial data points on Figure 13 form an approximate half-slope line and are assumed to indicate the presence of a fracture. Figure 14 presents the square root plot of this data; it is observed that the initial points on this graph also form a straight line with slope,  $m_1$ , equal to 103  $\text{psi/hr}^{1/2}$ .

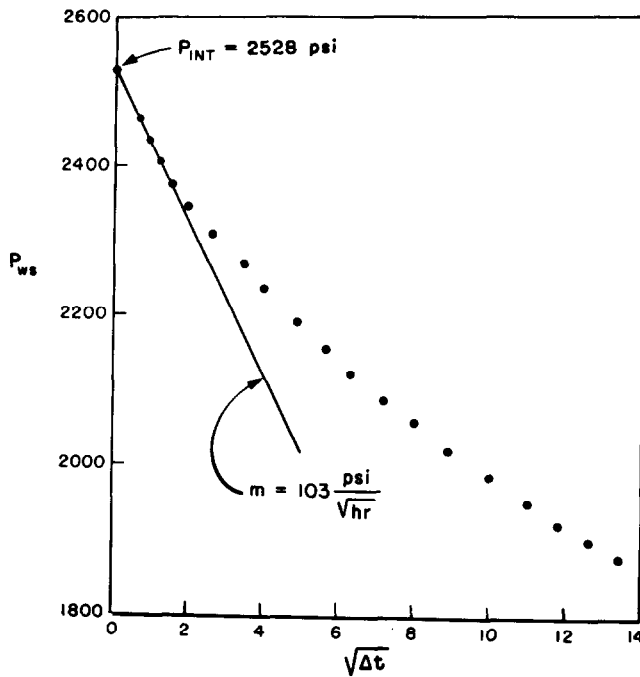


FIGURE 14 - SQUARE ROOT PLOT FOR EXAMPLE PROBLEM

From experience in the area, the fracture half length is believed to be approximately 175 ft. We use this as an initial estimate in Equation 16.

$$R = \exp \left[ -1.845 \left( \frac{175}{526} \right) \right]$$

$$R = 0.54$$

We substitute this information into Equation 17.

$$x_f = \frac{0.319}{103} \left[ \frac{(460)(350)(1)}{(0.08)(10 \times 10^{-6})(55)(0.54)} \right]^{1/2}$$

$$x_f = 254 \text{ ft}$$

Thus, the initial fracture length assumption appears too low.

This trial and error procedure is repeated until assumed and computed values of  $x_f$  are equal; these results are summarized in Table 2.

TABLE 2 SUMMARY OF FRACTURE LENGTH CALCULATIONS

$(x_f)_{\text{assumed, ft}}$	R	$(x_f)_{\text{calc, ft}}$
175	0.54	254
275	0.38	304
310	0.34	323
340	0.30	340

From Equation 15, we calculate the corrected permeability.

$$k = (0.30)(1.80) = 0.54 \text{ md}$$

Extrapolation of the straight line on Figure 14 to  $\Delta t^{1/2} = 0$  yields  $p_{\text{int}} = 2528$  psia. Equation 19 use provides the following.

$$S-S_{\text{frac}} = \frac{(2713-2528)(0.54)(55)}{(141.2)(460)(.8)(1.0)} \approx 0$$

Accordingly, it is concluded from Equation 6 that the damage skin factor is negligible.

The average reservoir pressure is determined from the Muskat plot. According to Equation 20, this method is valid for the following shut-in times.

$$\Delta t > \frac{(190)(0.08)(0.8)(10 \times 10^{-6})(20)(43.560)}{0.54}$$

$$\Delta t > 196 \text{ hours}$$

Figure 15 is a Muskat graph of the test data. It is observed that the late time data form a straight line for a minimum  $\bar{p}$  value of 1660 psia; accordingly, it is concluded that this is the volumetric average pressure associated with the injection well.

To summarize, conventional analysis indicates a formation permeability of 0.54 md, a fracture length of 340 ft, no formation damage, and a volumetric average reservoir pressure of 1660 psia.

An alternate method of analysis is to use type curves. Figure 11 is a generalized type curve for an infinite conductivity fracture. Figure 13 is the data curve. The match between the data curve and type curve is shown by Figure 16. From an arbitrary match point on Figure 16.

$$\Delta p_m = 100 \text{ psia} \quad p_{Dm} = 0.29$$

$$\Delta t_m = 100 \text{ hrs} \quad (\Delta t_{Dxt})_m = 1.30$$

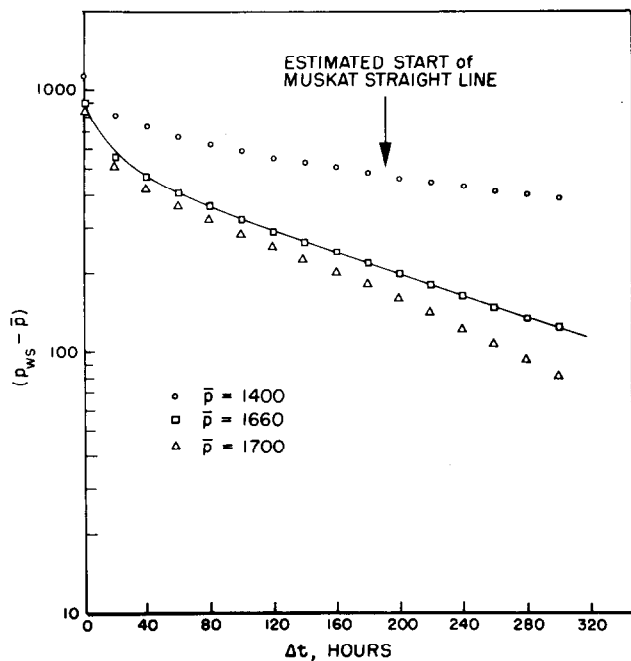


FIGURE 15—EXTENDED MUSKAT PLOT FOR EXAMPLE PROBLEM

From Equation 23,

$$k = \frac{(141.2) (350) (1) (0.8)}{(55) (100)} (0.29) = 2.1 \text{ md}$$

From Equation 24,

$$x_f = \left[ \frac{(0.000264) (2.1) (100)}{(0.08) (0.8) (10 \times 10^{-6}) (1.30)} \right]^{1.2}$$

$$x_f = 258 \text{ ft}$$

## FINITE CONDUCTIVITY FRACTURES

It is commonly observed, especially when working with massive hydraulic fractures, that fracture lengths computed in the previously described manner are much shorter than design lengths. This difference often represents several orders of magnitude. For example, a fracture designed to be 1000 feet long may be determined from pressure buildup testing to be 10 feet long. These discrepancies have led engineers to conclude that many fractures have a smaller flow capacity than can be adequately described by the infinite

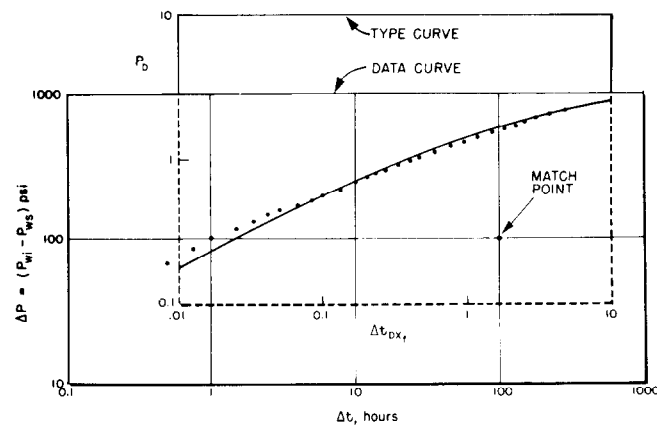


FIGURE 16—TYPE CURVE MATCH FOR EXAMPLE PROBLEM

capacity solutions. This is easily understood when one considers that a fracture with finite conductivity must be significantly longer than an infinite conductivity fracture to produce an equivalent effect on well test data.

Recognizing the inadequacy of infinite conductivity solutions for certain applications, researchers<sup>19, 20</sup> have developed type curve solutions for finite capacity fractures. Figure 17 presents the constant rate type curve developed by Agarwal, et al.<sup>20</sup> Like the infinite capacity type curve, these curves are dimensionless plots of pressure versus time; however this graph is complicated by an additional parameter, fracture capacity, which is defined as follows.

$$F_{cD} = \frac{k_f w}{k x_f} \quad (25)$$

It is obvious in Figure 17 that  $F_{cD}$  ranges from 0.1 to 500; values greater than approximately 500 represent an infinite capacity fracture. Significantly, Equation 25 shows that fracture capacity,  $k_f w$ , is not the only parameter that causes  $F_{cD}$  to be large; high values of  $F_{cD}$  may also be caused by low formation permeability and/ short fracture length.

The procedure required to use Figure 17 is the same as described for infinite conductivity solutions. However, there are problems which make use of this type curve difficult.

Practically speaking, it is difficult to obtain a unique solution for  $x_f$  and  $k$  using Figure 17. First, it is noted that the curves representing different

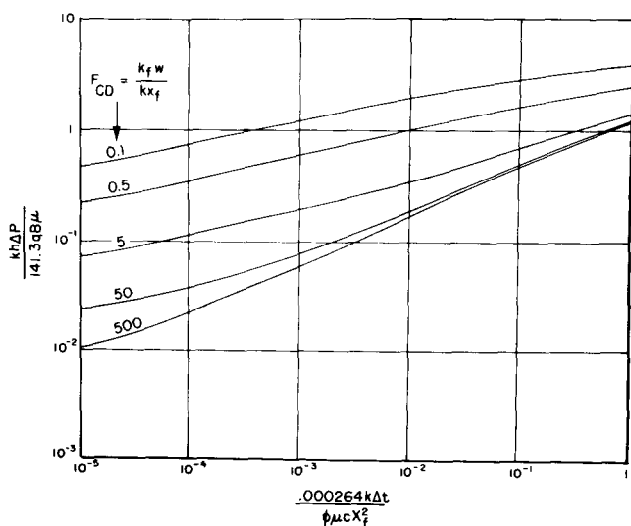


FIGURE 17—TYPE CURVE FOR FINITE CAPACITY VERTICAL FRACTURE. AFTER AGARWAL, ET AL.<sup>20</sup>

fracture capacities do not have distinct shapes; consequently, it is difficult to obtain a unique match. Second, it is observed that the curves all have slopes less than one-half; this is important because, as noted in our previous discussion, infinite conductivity fractures with skin may exhibit a similar shape. Accordingly, it is difficult to differentiate between finite capacity fractures and damaged infinite capacity fractures. Depending on the decision made, calculated results will differ significantly. Finally, if wellbore storage effects are present, the analysis is further complicated.

#### SUMMARY

Fractured reservoirs can be analyzed using pressure buildup tests to determine formation permeability, average formation pressure, formation damage and fracture length. The pressure behavior of a fractured well is significantly different from the radial flow behavior of homogeneous reservoirs. Consequently, conventional methods of pressure buildup analysis, based on radial flow theory, cannot be directly applied to these systems. The pressure behavior of a fractured well is dependent upon both the length and capacity of the fracture involved. An accurate analysis of a fractured well is only possible if first, it is recognized that the formation is fractured and, second, that some knowledge of fracture capacity is available.

When fracture capacity is large enough to be assumed infinite, early time buildup pressures

behave linearly and, in the absence of severe wellbore storage or skin effects, will plot as a straight line on a square root plot, and as a half-slope line on a log-log plot. These plots can be combined with a Horner graph to calculate permeability, skin and fracture length. This conventional method of fractured well analysis requires a trial-and-error procedure. Buildup data can also be analyzed using type curves; this method had the advantage of not requiring a trial-and-error calculation, but it does not yield any quantitative information about formation damage. The choice of conventional versus type curve analysis is a matter of personal preference since both methods give valid results.

Finite capacity fractures behave differently from infinite capacity fractures. Further, the pressure response of a well which intersects a finite-capacity fracture is dependent upon the magnitude of fracture capacity. Pressure tests from wells with finite-capacity fractures can only be analyzed using appropriate type curves.

A major difficulty in fractured well analysis is determining whether to use infinite-capacity or finite-capacity solutions to analyze the data. This is particularly true if the test data are altered by wellbore storage or skin effects. The behavior of the test data sometimes gives a clue as to the nature of the fracture: more often, however, the decision is not clear. Since computed results vary significantly depending upon the solution method used, it is concluded that we do not have the ability, with existing technology, to determine unique values of permeability and fracture length in most reservoirs.

#### NOMENCLATURE

- A = drainage area, sq ft
- $A_f$  = fracture face area, sq ft
- B = formation volume factor, RB/STB
- c = system compressibility,  $\text{psi}^{-1}$
- $F_{CD}$  = dimensionless fracture capacity
- FE = flow efficiency, dimensionless
- h = formation thickness, ft
- k = formation permeability, md
- $k_a$  = apparent formation permeability, md
- $k_f$  = fracture permeability

$m$  = slope (absolute value) of Horner straight line, radial flow, psi/cycle  
 $m'$  = maximum slope (absolute value) of Horner straight line, psi/cycle  
 $m_l$  = slope (absolute value) of linear flow straight line on square root plot, psi/hr<sup>1/2</sup>  
 $\bar{p}$  = average reservoir pressure, psia  
 $p^*$  = false pressure from Horner plot, psia  
 $p_{wi}$  = injection pressure at shut-in, falloff test, psia  
 $p_{wf}$  = flowing wellbore pressure at shut-in, psia  
 $p_{ws}$  = shut-in wellbore pressure, psia  
 $p_{int}$  = pressure at  $\Delta t^{1/2} = 0$ , square root plot, psia  
 $p_D$  = dimensionless pressure  
 $\Delta p_{skin}$  = skin pressure loss, psi  
 $q$  = flow rate, STB/D  
 $R$  = correction factor, dimensionless  
 $r_w$  = wellbore radius, ft  
 $s$  = skin factor, dimensionless  
 $t$  = producing time prior to shut-in, hrs  
 $\Delta t$  = shut-in time, hrs  
 $\Delta t_D$  = dimensionless shut-in time based on fracture half length  
 $w$  = fracture width, ft  
 $x_c$  = drainage radius, ft  
 $x_f$  = fracture half length, ft  
 $\phi$  = porosity, fraction  
 $\mu$  = viscosity, cp  
 $Exp$  = exponential of natural logarithm

## REFERENCES

1. Matthews, C.S. and Russell, D.G.: *Pressure Buildup and Flow Test in Wells*, Monograph Series, Society of Petroleum Engineers of AIME, Dallas (1967) 1.
2. Earlougher, Robert C., Jr.: *Advances in Well Test Analysis*, Monograph Series, Society of Petroleum Engineers of AIME, Dallas (1977) 5.
3. Ramey, H.J., Jr., Kumar, A., and Gulati, M.S.: *Gas Well Test Analysis Under Water Drive Conditions*, AGA, Arlington, Va. (1973).
4. Dyes, A.B., Kemp, C.E., and Caudle, B.H.: "Effect of Fractures on Sweep-out Patterns," *Trans AIME* (1958) 213, 245.
5. Prats, M., Hazebroek, P., and Stickler, W.R.: "Effect of Vertical Fractures on Reservoir Behavior - Compressible Fluid Case," *Soc. Pet. Eng. J.* (June, 1962) 87.
6. Scott, J.O.: "The Effect of Vertical Fractures on Transient Pressure Behavior of Wells," *J. Pet. Tech.* (Dec. 1963) 1365.
7. Horner, D.R.: "Pressure Buildup in Wells," *Proc. Third World Pet. Cong.*, The Hague (1951) Sec. II, 503.
8. Miller, C.C., Dyes, A.B., and Hutchinson, C.A., Jr.: "The Estimation of Permeability and Reservoir Pressure from Bottom Hole Pressure Buildup Characteristics," *Trans. AIME* (1954) 201, 182.
9. Matthews, C.S., Brons, F., and Hazebroek, P.: "A Method for Determination of Average Pressure in a Bounded Reservoir," *Trans. AIME* (1954) 201, 182.
10. Russell, D.G., and Truitt, N.E.: "Transient Pressure Behavior in Vertically Fractured Reservoirs," *J. Pet. Tech.* (Oct., 1974) 1159.
11. Clark, K.K.: "Transient Pressure Testing of Water Injection Wells," *J. Pet. Tech.* (June, 1968) 639.
12. Millheim, K.K., and Cichowicz, L.: "Testing and Analyzing Low-Permeability Fractured Gas Wells," *J. Pet. Tech.* (Feb. 1968) 193.
13. Wattenbarger, R.A., and Ramey, H.J., Jr.: "Well Test Interpretation of Vertically Fractured Gas Wells," *J. Pet. Tech.* (May, 1969) 625.
14. Agarwal, R.G., Al-Hussainy, R. and Ramey, H.J., Jr.: "An Investigation of Wellbore Storage and Skin Effect in Unsteady Liquid Flow: I. Analytical Treatment," *Trans. AIME* (1970) 249, 279.
15. Raghavan, R., Cady, G.V., and Ramey, H.J., Jr.: "Well Test Analysis for Vertically Fractured Wells," *Trans. AIME* (1972) 253, 1014.
16. Gringarten, A.C., Ramey, H.J., Jr., and Raghavan, R.: "Unsteady-State Pressure Distributions Created by a Well with a Single Infinite Conductivity Vertical Fracture," *Trans. AIME* (1974) 257, 347.
17. Gringarten, A.C., and Ramey, H.J., Jr.: "Unsteady State Pressure Distributions Created by a Well With a Single Horizontal Fracture, Partial Penetration, or Restricted Entry," *Trans. AIME* (1974) 257, 413.
18. Gringarten, A.C., Ramey H.J., Jr. and Raghavan, R.: "Applied Pressure Analysis for Fractured Wells," *Trans. AIME* (1975) 259, 887.
19. Cinco, H.L., Samaniego, F.V. and Dominguez, N.A.: "Transient Pressure Behavior for a Well With a Finite-Conductivity Vertical Fracture," *Soc. Pet. Eng. Jour.* (Aug., 1978) 253.
20. Agarwal, R.G., Carter, R.D. and Pollock, C.B.: "Evaluation and Prediction of Performance of Low Permeability Gas Wells Stimulated by Massive Hydraulic Fracturing," SPE 6838, Presented at 52nd Annual Technical Conference and Exhibition of the Society of Petroleum Engineers, Denver (Oct. 9-12, 1977).

21. Van Everdingen, A.F.: "The Skin Effect and Its Influence on the Productive Capacity of a Well," *Trans. AIME* (1953) 198, 171.
22. Hurst, W.: "Establishment of the Skin Effect and Its Impediment to Fluid Flow into a Wellbore," *Pet. Eng.* (Oct., 1953) 25, B-6.
23. Raghavan, R.: "Some Practical Considerations in the Analysis of Pressure Data," *Trans. AIME* (1976) 262, 1256.
24. Muskat, M.: "Use of Data on the Buildup of Bottom-hole Pressures," *Trans. AIME* (1937) 123, 44.

